Proceedings World Geothermal Congress 2026
Calgary, Canada, June 8 – 11, 2026

Coastal Effects in Magnetotelluric Geothermal Prospecting: Revisiting Deep Conductors in Iceland

Kristján Ó. Klausen[1,2]*, Léa Lévy[2,3], Egill Árni Guðnason[2], Arnar Már Vilhjálmsson[2] and Gylfi Páll Hersir[2]
University of Iceland[1]*, Iceland GeoSurvey[2], Géosciences Rennes, INSU, CNRS, France[3]
kristjank@hi.is

Keywords: Coastal effect, Resistivity, Electromagnetic methods, Magnetotellurics, Bathymetry

ABSTRACT

Along with transient electromagnetics (TEM), the magnetotelluric (MT) method has been applied in recent decades to image subsurface resistivity, with deep conductive bodies frequently observed extending into geothermal reservoirs. However, acute resistivity contrasts close to shorelines significantly affect MT data: the measured responses may become significantly distorted compared to a forward response that would not account for this effect. This has the potential to bias the inverted resistivity features, which may result in hiding deeper subsurface features and obstruct geothermal exploration. In this work, the coastal effect is briefly reviewed and cases from geothermal prospecting in Iceland are discussed. Although the coastal effect is well understood in theory, its influence on more recent electromagnetic methods has not been fully explored in Icelandic geothermal contexts, since the increasing availability of high-resolution seafloor models, along with improved numerical tools, offers new opportunities to revisit and better understand these effects. This contribution provides a brief conceptual overview of the coastal effect, supported by forward modeling, illustrating how underlying low-resistivity structures could be masked in some cases. The results show how both past and future near-shore MT soundings can benefit from implementation of high-resolution bathymetric data.

1 INTRODUCTION

Recently, two new low-temperature geothermal systems were found in Iceland close to the coastline (Cariaga, 2024ab). In both areas, earlier geophysical exploration by electromagnetic methods did not indicate underlying geothermal resources, which can be partially explained by the costal effect (Lilley, 2007). When exploration is carried out with direct-current electromagnetic methods, the highly conductive seawater draws the ground currents towards it, skewing the electrical measurements (Hersir, 1988). With the advent of more economical drilling, application of temperature gradient drilling, in conjunction with geological fault and fracture mapping, has mostly replaced direct-current methods in geophysical exploration in Iceland.

For alternating-current methods, such as Magnetotellurics (MT), the effects are more complicated due to electromagnetic induction (Chave, 1983). The influence of the shoreline on MT is commonly known as the coast/al effect (Key and Constable, 2011; Pandey *et al*., 2008), although related literature also refers to it as the geomagnetic coast effect (Parkinson and Jones, 1979; Petereit *et al*. 2022), peninsula effect or island effect (Lauritsen, 2016). Induction of electrical currents in both the ground and ocean is governed by Faraday's law, whereby a time-varying magnetic field induces electric field circulation, driving electrical currents, which in turn generate secondary induced magnetic fields (Maus, 2007).

Along with transient electromagnetics (TEM), magnetotelluric (MT) methods have been applied in recent decades to facilitate the exploration of high-enthalpy geothermal reservoirs, with typical resistivity signatures repeatedly imaged at various geothermal sites in the world (Árnason *et al.,* 2025; Samrock *et al.*,2018; Didas *et al.,* 2024; Gresse *et al.,* 2021). Thanks to the availability of new high-resolution seafloor models, along with improved numerical tools, the coastal effect can now be modelled more precisely. Here we explore here the possibility that the coastal effect may have distorted deeper resistivity structures.

We estimate the extent to which conductive structures in the depth range 2-5 km can be resolved using existing networks of MT measurements with or without modelling the coastal effect in the forward operator. We focus here on a synthetic analysis that helps better understand the importance of inversion settings and influence of the ocean, depending on the proximity to the coastline.

2 3-D INVERSION SETTINGS

3-D inversion techniques have become widely used in magnetotelluric (MT) data interpretation. However, with real data sets, many settings that control the outcome of 3-D inversion have not been sufficiently explored, such as alignment of the coordinate system, handling of data errors and model regularization (Tietze & Ritter, 2013). Here we summarize some of the most important findings in the literature with regards to choosing appropriate settings for 3-D inversion, before we explore in more detail the influence of including the bathymetry in the model and the forward calculations. We focus on 3-D inversion with the ModEM package (Egbert & Kelbert, 2012).

2.1 Principles of the ModEM solver

The inversion algorithm is based on a standard minimum-structure non-linear conjugate gradients algorithm. Within the inversion process, the ModEM-3DMT algorithm seeks to minimize the penalty function Φ, which consists of a data regularization and a model regularization term (Egbert & Kelbert, 2012; Kelbert *et al*., 2014):

$$\Phi(\mathbf{m},\mathbf{d}) = (\mathbf{d} - \mathbf{f}(\mathbf{m}))^{\mathrm{T}}\,\mathrm{C_d}^{-1}\,(\mathbf{d} - \mathbf{f}(\mathbf{m})) + \nu\,(\mathbf{m} - \mathbf{m}_0)^{\mathrm{T}}\,\mathbf{C_m}^{-1}\,(\mathbf{m} - \mathbf{m}_0) \qquad (1)$$

where **d** is the observed data, **m** the conductivity model, **f**(**m**) the forward response, $\mathbf{C}_d$ the data covariance, $\mathbf{m}_0$ the prior model, $\mathbf{C}_m$ the model covariance and *v* a trade-off parameter. The data covariance is a diagonal matrix, which contains the inverse of the squared data errors $\mathbf{e}_i$ for each data point: $\mathbf{C}_d=\mathrm{diag}(\frac{1}{e_i^2})$. The model covariance $\mathbf{C}_m$ is a 3-D smoothing and scaling operator, similar to the scheme used by Siripunvaraporn & Egbert, (2000). The model covariance $\mathbf{C}_m$ is applied to the distance of the current model **m** to the *a priori* model $\mathbf{m}_0$; in other words, the ModEM algorithm attempts to minimize differences in resistivity between the recovered model and the prior model (Lee *et al*., 2020). Hence, prior model properties and smoothing parameter settings are closely interrelated. In addition, in model cells where the sensitivity is low, the inversion model tends to remain at the assumed prior resistivities (Tietze & Ritter, 2013).

2.2 Model regularization settings

The covariance matrix C_m is used for model regularization and is defined in the ModEM software by the smoothness factors, with values between 0 and 1. Horizontal and vertical smoothing may be different, and the extent of horizontal smoothing may vary with depth, in both X and Y directions (Kelbert *et al*., 2014).These coefficients have an impact on the smoothness of solution. Small values allow for more rapid changes of the resistivity in the obtained model. Large coefficients limit contrasts of resistivity in neighboring cells and can produce models in which conductive areas are too big and with a respectively smaller conductivity (Slezak *et al*., 2019).

If deviations from a prior model are heavily penalized, regularization is prone to result in erroneous and misleading 3-D inversion models, particularly in the presence of strong conductivity contrasts. A ‘good’ overall rms misfit is often meaningless or misleading as a huge range of 3-D inversion results exist, all with similarly ‘acceptable’ misfits but producing significantly differing images of the conductivity structures. Reliable and meaningful 3-D inversion models can only be recovered if data misfit is assessed systematically in the frequency–space domain (Tietze & Ritter, 2013).

2.3 Diagonal and off-diagonal components and data weighting

According to (Tietze & Ritter, 2013), 2-D subsurface structures can vanish if data are not aligned with the regional geological strike direction, when interdependencies between data components are not considered in standard 3-D MT inversion codes. While integrating *Zxx* and *Zyy* (diagonal components) into the data set may degrade the performance of the inversion, due to the lower magnitudes and, therefore, lower signal-to-noise ratios of these elements, they might be important to consider. In this case, data weighting, that is, how strongly individual components of the impedance tensor and/or vertical magnetic field transfer functions dominate the solution, is a crucial control for the outcome of 3-D inversion. A small weight (large error) on diagonal components will tend to an inversion result where these components are ignored and thus can lead to biases, while a large weight (small error) may prevent the inversion procedure to converge.

Data weights and errors are handled very differently by various authors: statistically determined variances of the impedance tensor elements, impedance variances combined with pre-set error floors, or use of relative error bounds - i.e. a percentage of the data value (Tietze & Ritter, 2013). To resolve a deep conductor with inversion of impedances in the geographic north (N00°) aligned coordinate system, Tietze & Ritter (2013) tried to amplify the information contained in the smaller-sized diagonal impedance elements by setting their error bounds to very small values (e.g. a floor <1%$\sqrt{abs(\det(Z))}$. However, they also acknowledge that it is often not feasible to set

Zxx and *Zyy* errors to such small values for the entire period range, because the diagonal components of field data often suffer from poor signal-to-noise ratios, particularly in noisy environments. At the same time, defining large error bounds or using (large) statistically derived error bars, effectively downweights or omits the information contained in the diagonal impedance elements (Tietze & Ritter, 2013).

A series of tests were carried out to find out suitable error levels. For example, attempts were made to calculate error differently on the diagonal components (Zxx and Zyy) than on the off-diagonal components (Zxy and Zyx). This resulted in inversions not able to move forward. The best option was found to be, for all components, the following formula, as suggested by ModEM supporting software, 3D Grid:

$$Err = 5\%\sqrt{abs(Zxy \cdot Zyx)} \quad (2)$$

The resulting error on the off-diagonal components typically represents 5% of the value of these components. On the other hand, since the diagonal components are usually several orders of magnitude smaller than the off-diagonal, this formula results in errors on the diagonal components often higher than the values themselves. This means that the weight on the diagonal components in the inversion is very small, i.e. these components are not really being fitted by the procedure. This approach seems consistent with findings from the literature that diagonal components have a small signal-to-noise ratio. However, this aspect should be taken into consideration when interpreting results from real data sets.

3 INFLUENCE OF THE OCEAN

In order to assess the influence of the ocean on the ability to detect deep conductive structures through MT data modelling, two geothermal areas were investigated: Nesjavellir (relatively far from the coast) and Reykjanes proper (surrounded by coast line). Forward simulations were carried out, with and without bathymetry information included. Two types of models were tested: a homogeneous model for all Iceland (10 Ωm) and a typical resistivity structure of geothermal areas localized at each of the site, with both a shallow and deep conductor. The homogeneous models are illustrated in Figure 2 and the resistivity structures used in the analyses at Hengill and Reykjanes are represented in Figure 3.

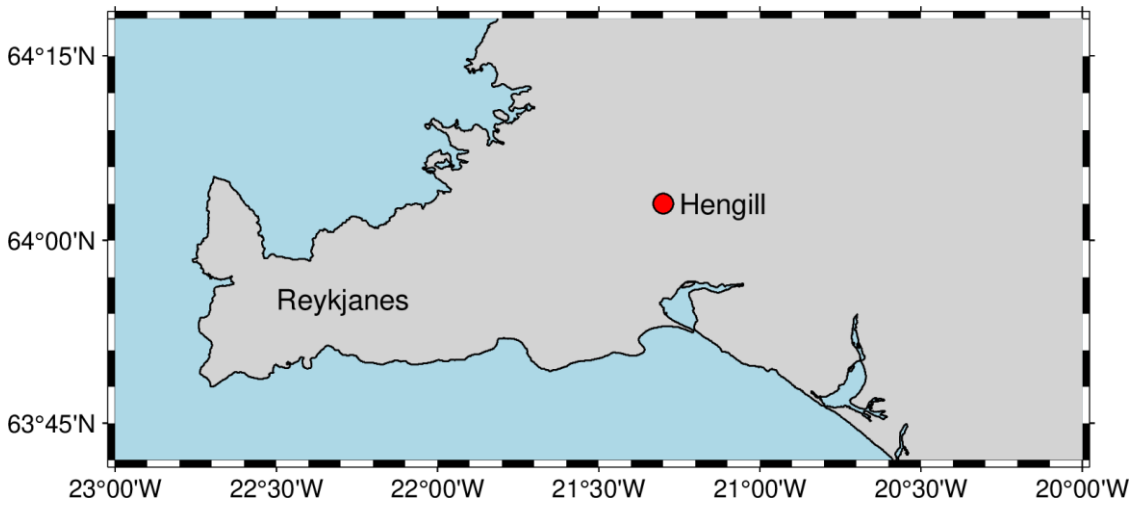


Figure 1. Southwest corner of Iceland showing Reykjanes Peninsula and Hengill volcano.

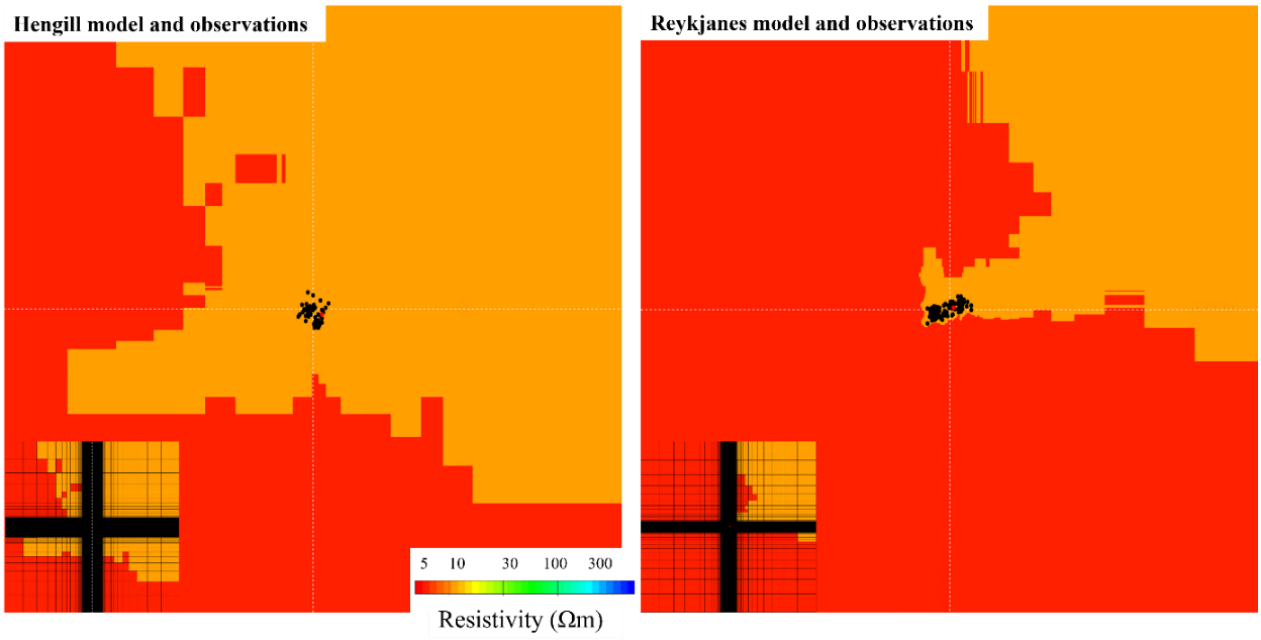


Figure 2. Homogeneous models (10 Ωm + ocean at 0.3Ωm) used in the analyses at Hengill (left) and Reykjanes (right). The mesh grids are further illustrated on the insets.

Six forward datasets were thus simulated: Reykjanes and Hengill, homogeneous and geothermal structure, bathymetry or no bathymetry. The synthetic dataset corresponding to the resistivity structure at Reykjanes, including bathymetry, was further inverted.

3.1 Forward simulations

The forward simulation of these synthetic cases are carried out with a model grid composed of 172 x 232 x 48 cells (X, Y, Z). The inner part comprises a uniform mesh of 130 × 190 × 48 cells (X Y Z) with an edge length of 109 m. On all four sizes, the central domain is padded with 21 planes where cell sizes increase laterally by a factor of 1.3. The vertical thickness is 50 m for the first layer; subsequent layer thicknesses successively increase by a factor of 1.2.

As expected, forward simulations illustrate a much stronger effect of the bathymetry in Reykjanes (Figure 4) than in Hengill (Figure 5). In Reykjanes (Figure 4), the effect also varies depending on the sounding location. It can be seen, e.g., that the bathymetry is causing a larger separation of the Zxy and Zyx components for soundings RKN151 and RKN152 (center and bottom panels) than for sounding RKN100 (top panel). In Hengill (Figure 5), the effect is slightly more significant in the southern part of the investigated area, possibly due to its greater proximity to the southern shore.

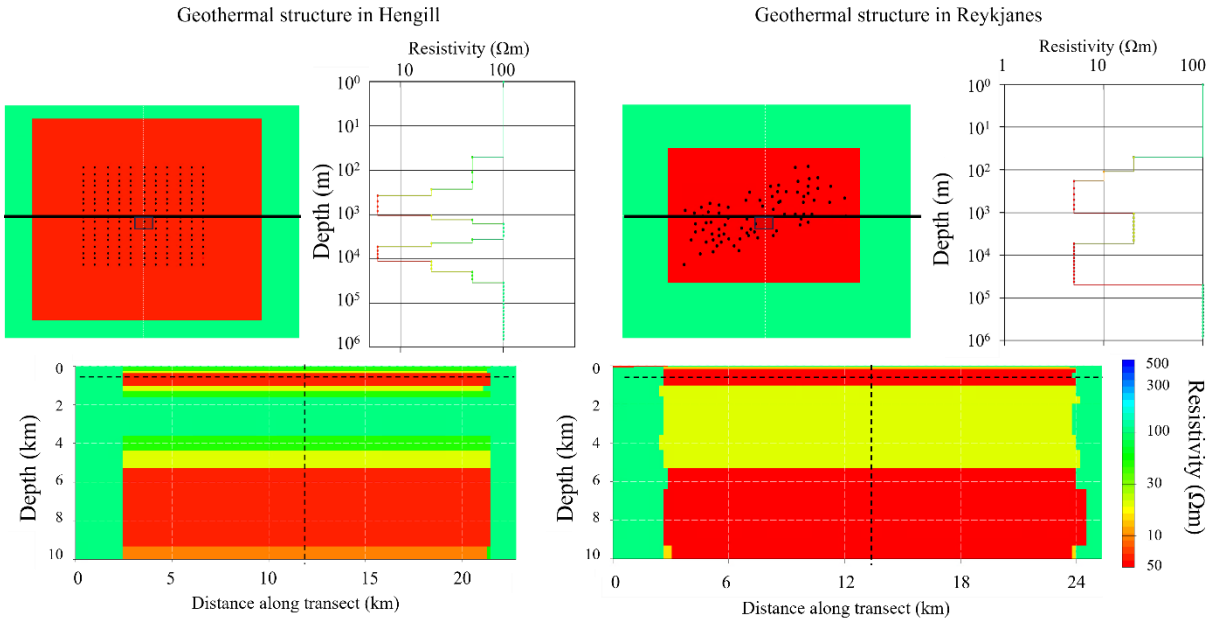


Figure 3. Resistivity structures used in the analyses at Hengill (left) and Reykjanes (right) to represent the typical signature of a geothermal system. Three views are shown: 2D slice at 500 m depth, 1D model and 2D transect. Their respective locations are indicated by dashed lines, square and plain lines.

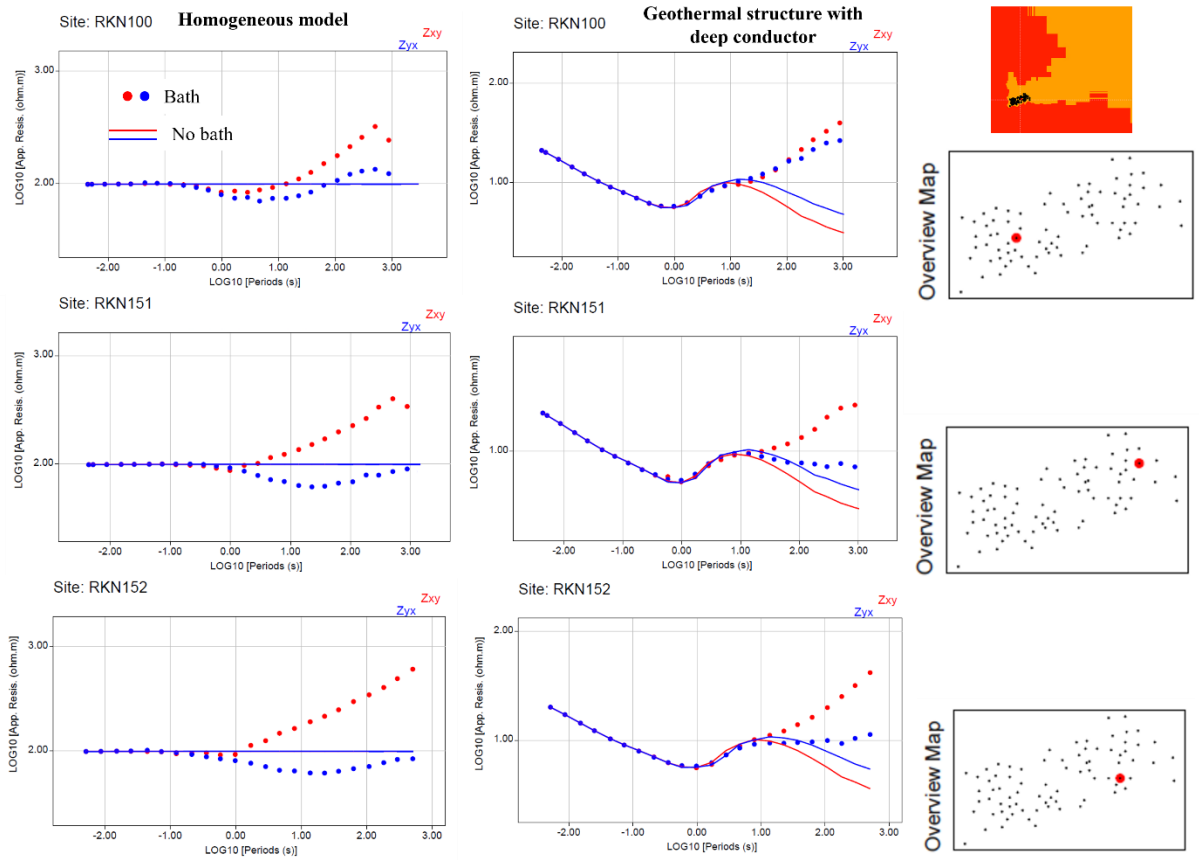


Figure 4. Forward simulations at Reykjanes, including bathymetry, using a homogeneous model at 100 Ωm (left panels) and a 1D model including both a shallow and deep conductor (right panels). The location of the soundings is shown as a red dot to the right.

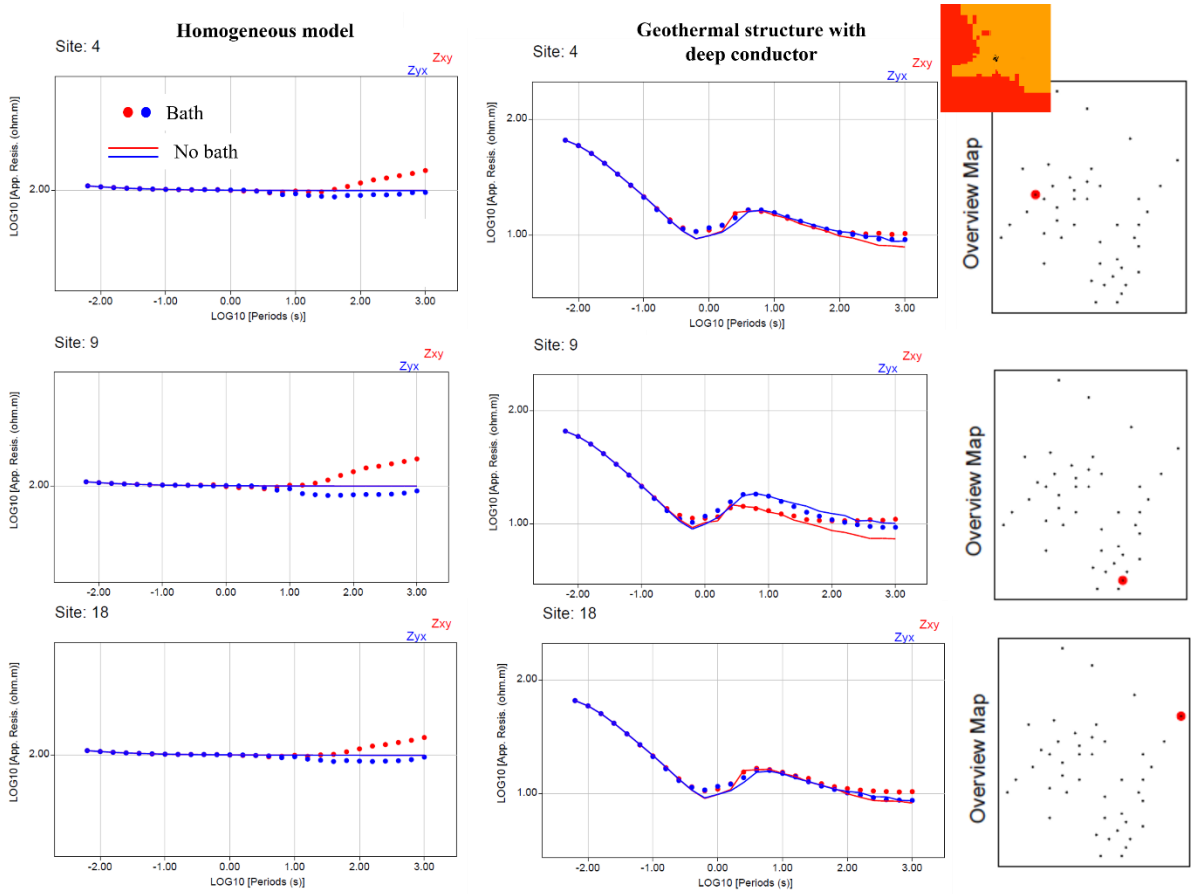


Figure 5. Forward simulations at Hengill, including bathymetry, using a homogeneous model at 100 Ωm (left panels) and a 1D model including both a shallow and deep conductor (right panels). Results are presented for three stations at Hengill: 4, 9 and 18, showing overall small effects from the ocean. The location of the soundings is shown as a red dot to the right.

These findings are in-line with Arafat and Daud (2020), where the greatest influence of the coastal effects is for periods of 1s and above, and as a rule of thumb, the effect is pronounced when the distance to the ocean is equal or less than the exploration depth for the given period/frequency. Comparison between the panels of Figure 3, also shows how skewing of the components varies between sites, both Z_{xy} and Z_{yx} being skewed upwards in one instance (RKN100), in which case using the determinant for a 1D model would lead to a significantly altered result.

3.2 Inversion

Inversion of the synthetic dataset corresponding to the reference model including the shallow and deep conductor (i.e. typical geothermal structure) was carried out at Reykjanes, with bathymetry. A 3-D bathymetry of the Icelandic shelf was included as *a priori* information. A resistivity of 0.3 Ωm was assigned to the sea water and this model domain was kept fixed at all times during the inversion. The remaining 'land cells' were set to 10 Ωm in the prior (and starting) model. Random noise of 5% was added to the data before inversion and data errors were set to 5% of $\sqrt{abs(Zxy * Zyx)}$ for both diagonal and off-diagonal impedance tensor elements.

It is observed in *Figure 6* that the shallow conductor and intermediary resistive layer are well resolved by the inversion, both in terms of value and thickness. The deep conductor on the other hand is not resolved at all: all inverted values below the intermediary resistor are equal to the prior. It can also be noted that the upper resistive layer (top 100 m, mostly visible on the 1D plot where the depth is shown with a log scale) is not resolved either but this is expected given its very small thickness when looking at it with a linear depth scale (2D transect).

In light of this result, it is worth considering if the absence of the deep conducting layer in south Iceland (Árnason *et al.* 2025 and references therein) could be explained by the coastal effect, given the short distance from the coast to the end of the coastal shelf.

In order to reach the convergence criterion (rms <1.05), the inversion had to be launched twice, with the second run using as a prior model the final inverted model of the first run. The rms of the final model in the first run was 1.53, meaning that the process stopped before reaching th convergence criterion. Using it as a prior model helped the inversion continue as it released the constraints on the homogeneous prior. A decent fit to the data is obtained (Figure 7), although further optimizing the inversion settings may help build more trust in the conclusions.

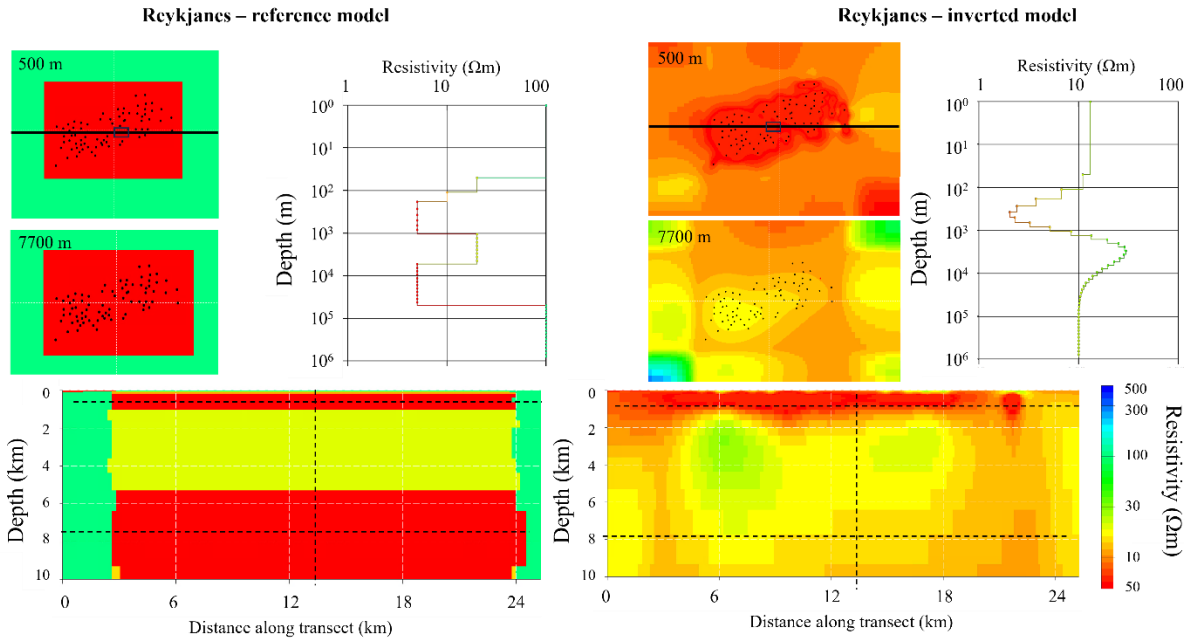


Figure 6. Reference model (left) versus inverted model (right) at Reykjanes, using the case where bathymetry is included. The prior and starting models were a homogeneous land at 10 Ωm, with seawater above bathymetry levels. 2D slices at 500 m and 7700 m are shown, corresponding to the shallow and deep conductor, respectively, in the reference model.

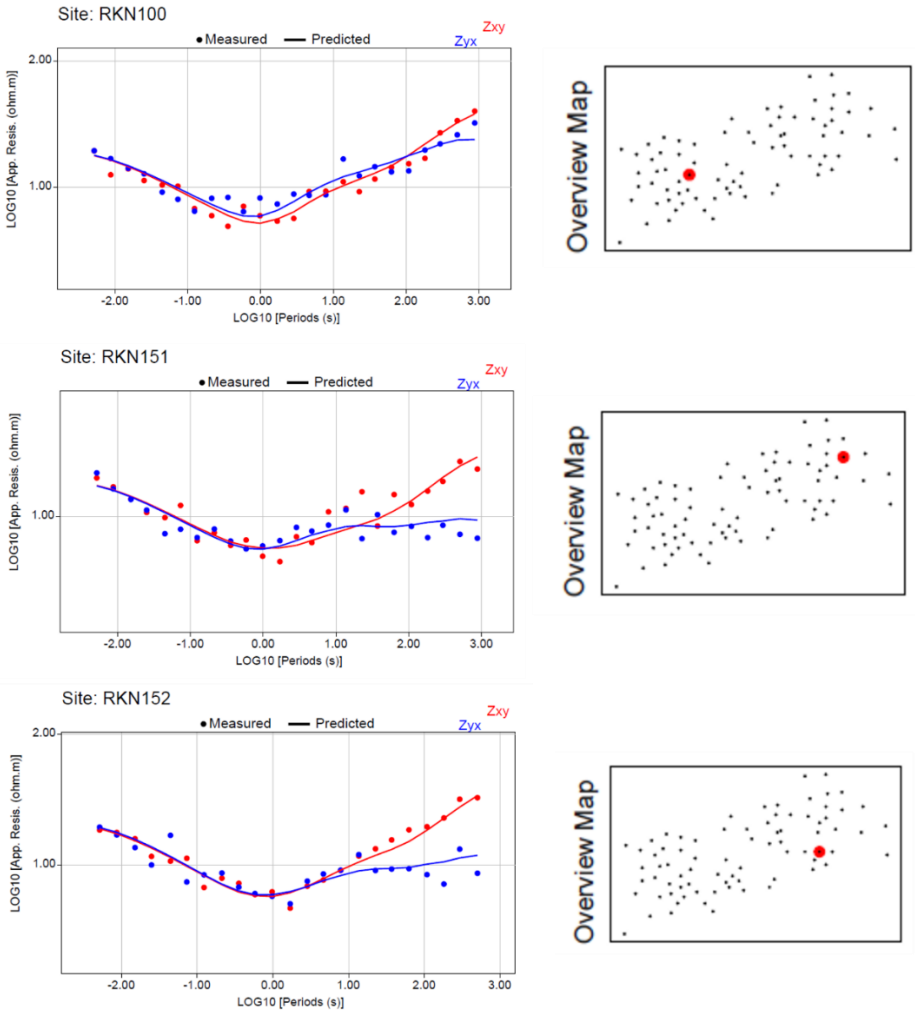


Figure 7. Data fit at three sites (the same as in Figure 4) in Reykjanes for the inversion shown in Figure 6.

4 CONCLUSIONS

A series of synthetic analyses were carried out in this study, using typical MT configurations used at Reykjanes and Hengill geothermal sites, Iceland, and the 3-D inversion software ModEM – Mod3DMT. The importance of different inversion settings was discussed, based on findings in the literature as well as synthetic tests and experience. The effect of the proximity to the shoreline on the ability to image the deep conductor, and thus recover the important features for geothermal exploration, was investigated. The results show how the seawater-land interface, represented by bathymetric data, considerably influences the ability of MT to resolve deep low-resisitivity targets. When comparing data inverted with and without bathymetry at Reykjanes, in synthetic cases where a shallow and deep geothermal conductors are included in the reference model, we see that the bathymetry tends to mask the signal from the deep conductor, as it increases the apparent resistivity everywhere. Furthermore, when inverting this synthetic dataset, we were not able to identify the deep conductor, although the shallow conductor and intermediary resistive layers were properly resolved. This calls for a reevaluation of previous interpretation of resistivity data in Iceland close to the shore, and highlights the need of evaluating how and if a deep conductor can be imaged when MT stations are in proximity to the ocean.

Acknowledgements

This research was supported by the DEEPEN project (DErisking Exploration for geothermal Plays in magmatic Environments), and partially funded by the ERANET Cofund GEOTHERMICA (Project no. 731117).

REFERENCES

Arafat, Y., Daud, Y.: Coast effects on 3-D inversion of magnetotelluric data for geothermal exploration in East Flores, Indonesia. *IOP Conference Series: Earth and Environmental Science* (2020), 538, 012071.

Árnason, K., Gibert, B., Bouligand, C. Vilhjálmsson, A.M.: The deep conductive layer in the Icelandic crust. *Earth-Science Reviews* (2025), 270, 105198.

Cariaga, C.: New low-temperature geothermal resources found in Reykjavik, Iceland. Think Geoenergy (2024a). *https://www.thinkgeoenergy.com/new-low-temperature-geothermal-resources-found-in-reykjavik-iceland/*

Cariaga, C.: Test drilling for geothermal in Ísafjörður, Iceland yields encouraging results. Think Geoenergy (2024b). *https://www.thinkgeoenergy.com/test-drilling-for-geothermal-in-isafjordur-iceland-yields-encouraging-results/*

Chave, Alan D.: On the Theory of ElectromagneticIn induction in the Earth by Ocean Currents, Journal of Geophysical Research, Vol. 88 (1983), No. B4, 3531-3542.

Didas, M. M., Armadillo, E., Hersir, G. P., Cumming, W., Rizzello, D., Benediktsdóttir, Á., & Geirsson, H. New MT surveys and 3D resistivity imaging beneath the Ngozi-Rungwe volcanoes at the triple rift junction of the East African Rift System in SW Tanzania: support for integrated interpretations of geothermal conceptual models. *Geothermics*, *118* (2024), 102893.

Egbert, G. D., & Kelbert, A.: Computational recipes for electromagnetic inverse problems. Geophysical Journal International, 189 (2012), 251–267.

Gresse, M., Uyeshima, M., Koyama, T., Hase, H., Aizawa, K., Yamaya, Y., et al. Hydrothermal and magmatic system of a volcanic island inferred from magnetotellurics, seismicity, self-potential, and thermal image: An example of Miyakejima (Japan). *Journal of Geophysical Research: Solid Earth*, 126 (2021), e2021JB022034.

Hersir, G.P. Correcting for the coastal effect on the apparent resistivity of Schlumberger soundings. Reykjavík: *National Energy Authority*. Available at https://gogn.orkustofnun.is/Skyrslur/OS-1988/OS-88019.pdf

Kelbert, A., Meqbel, N., Egbert, G. D., & Tandon, K.: ModEM: A modular system for inversion of electromagnetic geophysical data. Computers & Geosciences, 66 (2014), 40–53.

Key, K., Constable, S.: Coast effect distortion of marine magnetotelluric data: Insights from a pilot study offshore northeastern Japan. Physics of the Earth and Planetary Interiors 184 (2011), 194-207.

Lauritsen, N.L.B.: Magnetotelluric investigation in West Greenland - considering the polar electrojet, ocean and fjords. Technical University of Denmark (2016).

Lee, B., Unsworth, M., Árnason, K., & Cordell, D.: Imaging the magmatic system beneath the Krafla geothermal field, Iceland: A new 3-D electrical resistivity model from inversion of magnetotelluric data. Geophysical Journal International, 220 (2020), 541–567.

Lilley, T. Coast Effect of Induced Currents. In: Gubbins, D., Herrero-Bervera, E. (eds) Encyclopedia of Geomagnetism and Paleomagnetism. Springer, Dordrecht (2007).

Pandey, D., Sinha, M., Macgregor, L., Singh, S.: Ocean coast effect on magnetotelluric data: A case study from Kachchh, India. Marine Geophysical Researches 29 (2008), 185-193.

Parkinson, W.D., and Jones, F.W.: The geomagnetic coast effect, Reviews of Geophysics, Vol. 17 (1979), No. 8, 1999–2015.

Petereit, J., Saynisch-Wagner, J., Morschhauser, A., Pick, L., Thomas, M.: On the characterization of tidal ocean-dynamo signals in coastal magnetic observatories. Earth, Planets and Space 74 (2022), 67.

S. Maus, Electromagnetic ocean effects, in Encyclopedia of Geomagnetism and Paleomagnetism, ed. by D. Gubbins, E. Herrero-Bervera (Springer, Heidelberg, 2007)

Samrock, F., Grayver, A. V., Eysteinsson, H., & Saar, M. O. Magnetotelluric image of transcrustal magmatic system beneath the Tulu Moye geothermal prospect in the Ethiopian Rift. *Geophysical Research Letters*, *45*(23) (2018), 12-847.

Siripunvaraporn, W., & Egbert, G.: An efficient data-subspace inversion method for 2-D magnetotelluric data. Geophysics, 65 (2000), 791–803.

Slezak, K., Jozwiak, W., Nowozynski, K., Orynski, S., & Brasse, H.: 3-D studies of MT data in the Central Polish Basin: Influence of inversion parameters, model space and transfer function selection. Journal of Applied Geophysics, 161 (2019), 26–36.

Tietze, K., & Ritter, O.: Three-dimensional magnetotelluric inversion in practice—The electrical conductivity structure of the San Andreas Fault in Central California. Geophysical Journal International, 195 (2013), 130–147. https://doi.org/10.1093/gji/ggt234